

# On chemical equilibrium in nuclear collisions

F. Becattini<sup>1</sup>, M. Gaździcki<sup>2</sup>, J. Sollfrank<sup>3</sup>

<sup>1</sup> INFN Sezione di Firenze, Largo E. Fermi 2, I-50125 Firenze, Italy (e-mail: becattini@fi.infn.it)

<sup>2</sup> Institut für Kernphysik, Universität Frankfurt, August-Euler-Strasse 6, D-60486 Frankfurt, Germany (e-mail: marek@ikf.uni-frankfurt.de)

<sup>3</sup> Fakultät für Physik, Universität Bielefeld, Universitätsstr. 25, D-33615 Bielefeld, Germany (e-mail: sollfran@physik.uni-bielefeld.de)

Received: 31 October 1997 / Published online: 26 February 1998

**Abstract.** The data on average hadron multiplicities in central A+A collisions measured at CERN SPS are analysed with the ideal hadron gas model. It is shown that the full chemical equilibrium version of the model fails to describe the experimental results. The agreement of the data with the off-equilibrium version allowing for partial strangeness saturation is significantly better. The chemical freeze-out temperature of about 180 MeV seems to be independent of the system size (from S+S to Pb+Pb) and in agreement with that extracted in  $e^+ + e^-$ ,  $p + p$  and  $p + \bar{p}$  collisions. The strangeness suppression is discussed at both hadron and valence quark level. It is found that the hadronic strangeness saturation factor  $\gamma_S$  increases from about 0.45 for  $p + p$  interactions to about 0.7 for central A+A collisions with no significant change from S+S to Pb+Pb collisions indicating that the strangeness enhancement in heavy ion collisions cannot be fully attributed to the increased system size. The quark strangeness suppression factor  $\lambda_S$  is found to be about 0.2 for elementary collisions and about 0.4 for heavy ion collisions independently of collision energy and type of colliding system.

## 1 Introduction

Many years of experimental effort in the field of high energy nuclear collisions yielded a large amount of data on particle production at different collision energies (up to 200 A GeV/c) and for different colliding systems [1]. These results allow studying the properties of strongly interacting matter at high energy densities. Ultimately, at high enough collision energy one expects to create in the laboratory the Quark-Gluon Plasma (QGP), a form of matter in which effective degrees of freedom are quarks and gluons instead of hadrons and hadronic resonances. The formation of QGP with deconfinement of quarks and gluons should hopefully be reflected in the final hadron production, provided that the expected modifications of the entropy and strangeness content of the system survive hadronization and reinteractions between final state hadrons. In principle the system evolution is determined by QCD. Nevertheless, the formation of hadrons is a process entirely lying in its non-perturbative domain, hence, in order to study the final state, one has to resort to phenomenological models such as string or statistical (thermal) models.

The statistical models, whose prototypes [2–4] date back to '50s and '60s, are based on the assumption of local filling of available phase space according to statistical laws, once collective effects have been taken into account. This *ansatz* allows the characterization of hadron produc-

tion by means of few parameters such as temperature, volume and chemical potentials. Furthermore, parameters accounting for possible departures from complete equilibrium are often introduced.

A long and rich history of thermal models is related to their surprising success in the description of many aspects of high energy collisions [5]. It has been shown recently that the ideal hadron gas model allowing for non-equilibrium strangeness abundance is able to reproduce hadron multiplicities in  $e^+ + e^-$ ,  $p + p$  and  $p + \bar{p}$  interactions over a large collision energy range [6–8]. In this paper we apply the same model to analyse the data of hadron multiplicities in central nucleus-nucleus collisions at CERN SPS collision energies. The data on Sulphur-nucleus collisions at 200 A GeV/c were already analysed using thermal models in many previous works (for a review see [9]). We add to this data set the preliminary results on hadron production in central Pb+Pb collisions at 158 A GeV/c. The use of the same formulation of the thermal model for the analysis of data from  $p + p$  to central Pb+Pb collisions allows us to study the evolution of the parameters of the model in the full range of the colliding systems. Our analysis is based on hadron multiplicities integrated over the full phase space because their use minimizes the influence of collective effects on final results allowing a formulation of the model to be tested with a minimal number of assumptions and parameters.

The paper is organized as follows: in Sect. 2 we describe the hadron gas model which is confronted with the experimental data in Sect. 3. Discussion and conclusions are given in Sect. 4.

## 2 Hadron gas model

In this section the hadron gas model used in the present analysis is sketched; a more detailed description can be found in [7, 8]. The model postulates the formation of an arbitrary number of hadron gas fireballs each having a definite collective momentum as the result of an interaction between the two colliding systems. The parameters describing a hadron gas fireball at thermal and chemical equilibrium are the temperature  $T_i$ , the volume  $V_i$  in its rest frame, and the quantum numbers, i.e. electric charge  $Q_i$ , baryon number  $B_i$  and strangeness  $S_i$ . Charm and beauty have been excluded from the calculations as the thermal production of heavy-flavoured hadrons is negligible with respect to non-heavy-flavoured hadrons in the expected range of temperatures, namely 100–200 MeV. If  $\mathbf{Q}_i^0 = (Q_i, B_i, S_i)$  is the vector of  $i^{\text{th}}$  fireball's quantum numbers and  $N$  is the number of fireballs, the following constraint:

$$\sum_{i=1}^N \mathbf{Q}_i^0 = \mathbf{Q}^0, \quad (1)$$

where  $\mathbf{Q}^0$  is the quantum vector fixed by the initial state, must be fulfilled. The average yield of any hadron in the  $i^{\text{th}}$  fireball can be derived from the partition function:

$$Z_i(\mathbf{Q}_i^0) = \sum_{\text{states}} e^{-E_i/T_i} \delta_{\mathbf{Q}_i, \mathbf{Q}_i^0}, \quad (2)$$

which is calculated in the canonical approach, i.e. by using only the multi-hadronic states having the same quantum numbers of the fireball.

A non-equilibrium parameter  $\gamma_{S_i}$  accounting for a possibly incomplete strangeness chemical equilibration is introduced by multiplying by  $\gamma_{S_i}^s$  the Boltzmann factors  $e^{-E_j/T_i}$  associated to the  $j^{\text{th}}$  hadron in the partition function, where  $s$  is the number of its valence strange quarks and antiquarks. Although this factor was introduced heuristically [10] and used as a purely phenomenological parameter in the analysis of elementary collisions [6–8], it can be shown that  $\gamma_S$  formally is the fugacity associated to the number of strange + antistrange quarks in the hadron phase in a grand-canonical framework [11].

The overall average multiplicity of each hadron species is the sum of all average yields in each fireball. In principle any configuration  $\{\mathbf{Q}_1^0, \dots, \mathbf{Q}_N^0\}$  of fireballs in the event may occur, so that average hadron abundances depend on the probability  $w(\mathbf{Q}_1^0, \dots, \mathbf{Q}_N^0)$  of occurrence of a given configuration besides the whole set of fireball thermal parameters  $T_i$ ,  $V_i$  and  $\gamma_{S_i}$ . However, it can be shown that if such configuration weights  $w(\mathbf{Q}_1^0, \dots, \mathbf{Q}_N^0)$  are chosen in a statistical fashion [7, 8]:

$$w(\mathbf{Q}_1^0, \dots, \mathbf{Q}_N^0) = \frac{\delta_{\sum_i \mathbf{Q}_i^0, \mathbf{Q}^0} \prod_{i=1}^N Z_i(\mathbf{Q}_i^0)}{\sum_{\mathbf{Q}_1^0, \dots, \mathbf{Q}_N^0} \delta_{\sum_i \mathbf{Q}_i^0, \mathbf{Q}^0} \prod_{i=1}^N Z_i(\mathbf{Q}_i^0)} \quad (3)$$

and the fireball freeze-out temperatures and  $\gamma_{S_i}$  suppression factors are the same, namely  $T_i \equiv T$  and  $\gamma_{S_i} \equiv \gamma_S$ , then the average hadron abundances  $n_j$  at freeze-out depend only on the *global volume*  $V \equiv \sum_{i=1}^N V_i$  and  $\mathbf{Q}^0$  through the following equation:

$$n_j = (2J_j + 1) \frac{VT}{2\pi^2} \times \sum_{l=1}^{\infty} (\mp 1)^{l+1} \frac{Z(\mathbf{Q}^0 - l\mathbf{q}_j)}{Z(\mathbf{Q}^0)} \gamma_S^{ls_j} \frac{m_j^2}{l} K_2\left(\frac{lm_j}{T}\right), \quad (4)$$

where the upper sign is for fermions and the lower for bosons; the function  $Z$  is the *global partition function* [7, 8] and  $\mathbf{q}_j$  is the quantum number vector of the  $j^{\text{th}}$  hadron species.

The special choice of weights  $w(\mathbf{Q}_1^0, \dots, \mathbf{Q}_N^0)$  in [7, 8] leads to the same expression of average multiplicities relevant to a system in global equilibrium even if the fireballs are not in mechanical equilibrium. It might be argued that the difference between the rapidity spectra of baryons and antibaryons – existing even in central A+A collisions [12] – question the validity of this choice. Nevertheless this choice has a remarkable property, namely it removes the dependence of hadron average multiplicities on both the number of fireballs and their ordering either in size or in space (reabsorbed in the global volume). As a consequence, much freedom is left to possibly reproduce the rapidity distributions within the model keeping the same quantitative expressions for hadron abundances (see Appendix A). However, even if the choice of the weights  $w(\mathbf{Q}_1^0, \dots, \mathbf{Q}_N^0)$  was not correct, the corrections to (4) are expected to be small because the relative abundances are predominantly determined by the intensive thermal parameters and not by fireball quantum configuration weighting.

The *chemical factors*  $Z(\mathbf{Q}^0 - l\mathbf{q}_j)/Z(\mathbf{Q}^0)$  in (4) implement the dependence of the yields upon the chemistry of the system and replace the chemical potentials in the proper canonical formalism. For very large volumes, as expected in heavy ion collisions, it can be proved [8] by means of a saddle-point approximation, that (4) reduces to:

$$n_j = (2J_j + 1) \frac{VT}{2\pi^2} \sum_{l=1}^{\infty} (\mp 1)^{l+1} \gamma_S^{ls_j} \frac{m_j^2}{l} K_2\left(\frac{lm_j}{T}\right) \times e^{l\mathbf{Q}^0 \mathbf{A}^{-1} \mathbf{q}_j / 2} e^{-l^2 \mathbf{q}_j \mathbf{A}^{-1} \mathbf{q}_j / 4}, \quad (5)$$

where  $\mathbf{A}$  is a  $3 \times 3$  matrix whose elements are proportional to  $V$ :

$$\mathbf{A}_{k,l} = \frac{1}{2} \sum_j \frac{V(2J_j + 1)}{(2\pi)^3} \times \int d^3p \frac{\gamma_S^{s_j} e^{-\sqrt{p^2 + m_j^2}/T}}{(1 \pm \gamma_S^{s_j} e^{-\sqrt{p^2 + m_j^2}/T})_2} q_{j,l} q_{j,k}, \quad (6)$$

where the sum runs over all hadron species. In (5) the chemical factors are transformed into a product of two factors: the first one can be written as  $\exp[l\boldsymbol{\mu} \cdot \mathbf{q}_j/T]$  where

$\mu$  is a traditional set of chemical potentials, whereas the factor  $\exp[-l^2 \mathbf{q}_j A^{-1} \mathbf{q}_j / 4]$  has no grand-canonical corresponding quantity. Its presence entails a suppression of hadrons having non-vanishing quantum numbers with respect to neutral ones, owing to the finite size of the system. Indeed this factor takes its origin from the requirement of exact conservation of initial quantum numbers. In the infinite volume limit  $A^{-1}$  goes to zero and the grand-canonical formalism is fully recovered.

An important problem to face in modelling heavy ion collisions is the fact that particle multiplicities are measured by averaging over events with a varying number of participant nucleons. For central collisions of identical nuclei (S+S and Pb+Pb in this paper) the fluctuations in the number of spectator nucleons,  $N_{\text{SPEC}}$ , can be considered to follow a Poisson distribution [13], well approximated by a Gaussian distribution if  $\langle N_{\text{SPEC}} \rangle \gg 1$ . Hence fluctuations in the number of participant nucleons,  $N_{\text{PART}} = 2 \cdot A - N_{\text{SPEC}}$ , can be described by a Gaussian distribution with mean value  $\langle N_{\text{PART}} \rangle$  and variance  $\langle N_{\text{SPEC}} \rangle$ . For the considered collisions (S+S and Pb+Pb<sup>1</sup>) it is  $\langle N_{\text{SPEC}} \rangle \ll \langle N_{\text{PART}} \rangle$ , implying that the mean of participant nucleons distribution is large in comparison with its width. Assuming that  $T$  and  $\gamma_S$  do not depend on the number of participant nucleons, the average number of directly produced hadrons of species  $j$  is:

$$\begin{aligned} \langle n_j \rangle &= (2J_j + 1) \sum_{\mathbf{Q}^0} \int dV F(\mathbf{Q}^0, V) \frac{VT}{2\pi^2} \\ &\times \sum_{l=1}^{\infty} (\mp 1)^{l+1} \gamma_S^{ls_j} \frac{m_j^2}{l} K_2 \left( \frac{lm_j}{T} \right) \\ &\times e^{l\bar{\mu} \cdot \mathbf{q}_j / T} e^{-l^2 \mathbf{q}_j A^{-1} \mathbf{q}_j / 4} \end{aligned} \quad (7)$$

where  $F(\mathbf{Q}^0, V)$  is the joint probability of observing an event with global volume  $V$  and quantum vector  $\mathbf{Q}^0$  (determined by the number of protons and neutrons involved in the collision). The removal of the integral from (6) by introducing mean chemical potentials  $\bar{\mu}$  and mean volume  $\bar{V}$  must be undertaken with great care since such mean values in general would depend on the hadron species and would not be the same for all of them. This is clearly understood because  $\mu$  and  $A$ , depending on  $\mathbf{Q}^0$  and  $V$ , multiply  $\mathbf{q}_j$  in a non-factorisable form. However, if a reasonable *ansatz* of a narrow Gaussian shape for the distribution function  $F(\mathbf{Q}^0, V)$  is assumed, according to previous discussion, it can be shown (see Appendix B) that the simple averaging procedure introducing mean chemical potentials and volume can be used provided that  $A^{-1} \ll 1$ . In other words, for the following simple averaging formula to hold:

$$\begin{aligned} \langle n_j \rangle &\approx (2J_j + 1) \frac{\bar{V}T}{2\pi^2} \sum_{l=1}^{\infty} (\mp 1)^{l+1} \gamma_S^{ls_j} \frac{m_j^2}{l} K_2 \left( \frac{lm_j}{T} \right) \\ &\times e^{l\bar{\mu} \cdot \mathbf{q}_j / T} e^{-l^2 \mathbf{q}_j \bar{A}^{-1} \mathbf{q}_j / 4}, \end{aligned} \quad (8)$$

<sup>1</sup> Validity of the above consideration for central S+Ag collisions is questionable as fluctuations are probably dominated by a geometrical effect.

a nearly grand-canonical regime and reasonably small fluctuations of  $V$  and  $\mathbf{Q}^0$  are needed. How small such fluctuations must be, will be checked *a posteriori* in the actually examined collisions. The hadron average multiplicities are calculated with (8) in which  $\bar{V}$ ,  $T$ ,  $\gamma_S$  and  $\bar{\mu}_B$  are free parameters to be fitted to the data, while  $\bar{\mu}_S$  and  $\bar{\mu}_Q$ , the strangeness and the electrical chemical potentials respectively, have been determined by means of two additional constraints: the strangeness neutrality and the conservation of the ratio  $(Z_1 + Z_2)/(A_1 + A_2)$  formed with the atomic and mass numbers of the two colliding nuclei:

$$\begin{aligned} \sum_j S_j \langle n_j \rangle &= 0 \\ \sum_j Q_j \langle n_j \rangle &= \frac{Z_1 + Z_2}{A_1 + A_2} \sum_j B_j \langle n_j \rangle. \end{aligned} \quad (9)$$

It should be noted that the first of the two constraints in (9) is valid on an event by event basis whereas the second, only averaged over a large number of collisions.

All previous equations are concerned with primary hadrons, namely particles and resonances directly emitted from the hadronic source and not coming from secondary decays. On the other hand, since actual measurements include feeding from heavier hadrons and resonances, the hadron production rates to be compared with the data have been calculated by letting all primary hadrons decay according to known branching ratios until particles considered stable by the experiments are reached. Among primary hadrons we included all particles and resonances up to a mass of 1.7 GeV; the masses of resonances have been distributed according to a relativistic Breit-Wigner. The needed values of hadron masses, widths and branching ratios have been taken from the most recent Particle Data Book [14].

## 3 Comparison with the data

### 3.1 Full equilibrium model

The hadron gas model described in the previous section has been used to fit the data on hadron abundances in central S+S, S+Ag at 200  $A$  GeV/ $c$  and central Pb+Pb collisions at 158  $A$  GeV/ $c$  measured by NA35 and NA49 Collaborations at CERN SPS. We used average hadron multiplicities measured in (or extrapolated to) full phase space. The compiled data and the references to the original papers, where the experimental details (acceptances, extrapolation procedures) can be found, are given in Table 1. Since preliminary data on central Pb+Pb collisions are still poor, we decided in this case to use in addition two particle ratios measured in the central rapidity region, namely  $K^+/K^-$  and  $\bar{A}/A$ . The measured rapidity distributions of these particles in the acceptance region are similar to those of the corresponding antiparticles [21], thus justifying our decision to use those ratios as estimates of the full phase space ones. The analysis of particle multiplicities in  $e^+ + e^-$ ,  $p + p$  and  $p + \bar{p}$  collisions within a

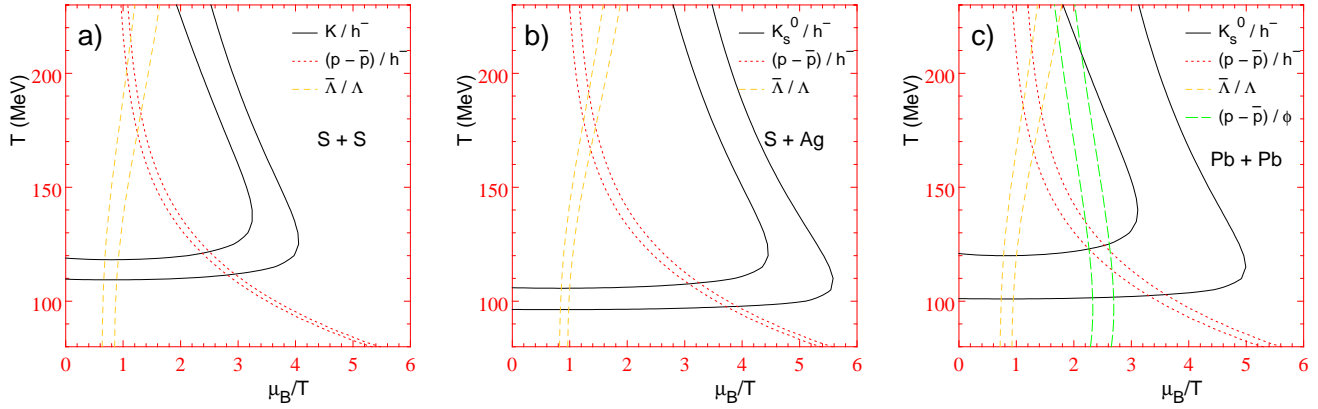


**Fig. 1.** Particle ratios in the grand-canonical approximation for  $\gamma_S = 1$ . The bands correspond to  $\pm 1\sigma$  deviations of the experimental ratios summarized in Table 1. The symbol  $K$  stands for  $\langle K \rangle = \langle K^+ \rangle + \langle K^- \rangle + 2\langle K_s^0 \rangle$

hadron gas model indicates that the strangeness production in such elementary collisions is not high enough to ensure the complete local chemical equilibrium at hadron level. It may be expected that in the case of central A+A collisions, due to a much larger volume of the interaction region and an increased role of hadron rescattering, a full local chemical equilibration at hadronic level can be attained.

In order to test this hypothesis we started the comparison of the experimental data with the hadron gas model by using first its fully equilibrated version, i.e. by setting  $\gamma_S = 1$ . We performed a graphical test similar to that made in [22] by plotting in the  $T$ - $\bar{\mu}_B/T$  plane the bands determined by the central values of some of the most relevant ratios of hadron yields and by their  $1\sigma$  variations. As the overall multiplicities are very large, we set  $A^{-1} = 0$  in (8); in this grand-canonical limit the multiplicity ratios depend only on the intensive free parameters  $T$  and  $\bar{\mu}_B/T$  as the mean volume  $\bar{V}$  cancels out. This approximation turns out to be satisfactory for all the examined collisions as it is demonstrated below. In Fig. 1 a–c such bands are shown for S+S, S+Ag and Pb+Pb data, respectively. There is no evident common crossing region for all bands, indicating absence of complete equilibrium even in central collisions of nuclei as heavy as Lead. It should be noted that a crossing region does exist for Pb+Pb collisions with  $T \simeq 120$  MeV and  $\bar{\mu}_B/T \simeq 2.7$ , as long as only full phase space multiplicities are considered, i.e. excluding the  $\bar{\Lambda}/\Lambda$  band. However, these latter values imply an antibaryon/baryon ratio of less than  $10^{-2}$  at primary level, which is unrealistically small with respect to the same ratio in S+S and S+Ag collisions. In fact the measured  $\bar{\Lambda}/\Lambda$  band is quite far from the crossing point.

In order to confirm the previous finding we performed a least-squared fit to the data with  $T$ ,  $\bar{V}$  and  $\bar{\mu}_B/T$  as free parameters, using the canonical corrections and keeping  $\gamma_S = 1$  fixed. The details of the fitting procedure are described in Appendix C. The results are shown in the first part of Table 2 and the fourth column of Table 1. The  $\chi^2/NDF$ 's are about  $6 \div 8$  with large discrepancies between fitted and measured values. Therefore we con-

clude that a full equilibrium version of the ideal hadron gas model fails to reproduce full phase space hadron multiplicities in central A+A collisions at CERN SPS energies.

Our conclusion is in contradiction with the findings in [23]. This discrepancy can be explained by the fact that the analysis in [23] was performed by using particle ratios in various regions of rapidity and transverse momentum which, unlike in our analysis, requires additional dynamical input beyond a simple statistical *ansatz*. Secondly, a proper statistical comparison between model predictions and data has not been performed in [23].

### 3.2 Off-equilibrium model

We tested the off-equilibrium version of the ideal hadron gas model repeating the fits with  $\gamma_S$  as a free parameter. The results of these new fits are shown in Table 1 and in the lower half of Table 2 while the comparison between fitted and measured multiplicities (or ratios) is shown in Table 1. There is a good agreement for all particles with some exceptions such as antiprotons in both S+S and S+Ag collisions. The  $\chi^2/NDF$  for S+S and S+Ag collisions is about 3.5, thus significantly lower than for the full-equilibrium fit. The  $\chi^2/NDF$  for central Pb+Pb collisions is close to 1.

The obtained temperatures and baryon chemical potentials are quite compatible with a common value and so are the  $\gamma_S$  values which turn out to be definitely less than 1 in all the three examined collisions. Also quoted in Table 2 are the obtained chemical potentials  $\bar{\mu}_S$  and  $\bar{\mu}_Q$  and the range of variation of the matrix  $A^{-1}$  elements; their smallness bears out the saddle-point approximation used in this analysis and the previously described graphical test by confirming the proximity to the grand-canonical regime.

### 3.3 Discussion of the analysis

The dependence of the fitted parameters on the hadron mass spectrum cut-off has been checked by repeating the fit with lower cut-off values and found to be negligible.

**Table 1.** Comparison between fitted and measured hadron abundances and ratios. All quoted multiplicities do not include feeding from weak decays unless otherwise stated. Note: the  $\chi^2$ 's calculated by using values quoted below differ from those of Table 2 as the latter include contribution from uncertainties on input hadron parameters

Hadron	Measured	Fitted	Fitted with $\gamma_S=1$	Reference
S+S collisions				
$h^-$ <sup>(a)</sup>	98±3	92.63	82.04	[15]
$K^+$	12.5±0.4	12.68	13.75	[16]
$K^-$	6.9±0.4	7.611	7.785	[16]
$K_s^0$	10.5±1.7	9.939	10.49	[12]
$\Lambda$ <sup>(b)</sup>	9.4±1.0	7.692	10.13	[12]
$\bar{\Lambda}$ <sup>(b)</sup>	2.2±0.4	1.474	2.825	[12]
$p-\bar{p}$ <sup>(c)</sup>	21.2±1.3	21.49	19.79	[15]
$\bar{p}$ <sup>(d)</sup>	1.15±0.4	2.092	2.314	[17]
S+Ag collisions				
$h^-$ <sup>(a)</sup>	186±11	171.3	147.2	[15]
$K_s^0$	15.5±1.5	17.43	19.44	[12]
$\Lambda$ <sup>(b)</sup>	15.2±1.2	13.99	17.44	[12]
$\bar{\Lambda}$ <sup>(b)</sup>	2.6±0.3	2.223	2.612	[12]
$p-\bar{p}$ <sup>(c)</sup>	43±3	43.44	39.18	[15]
$\bar{p}$ <sup>(d)</sup>	2.0±0.8	3.381	2.401	[17]
Pb+Pb collisions				
Net baryon	372±10	375.7	372.6	[18]
$h^-$ <sup>(a)</sup>	680±50	650.2	638.5	[19]
$K_s^0$	68±10	58.27	73.44	[19]
$\phi$	5.4±0.7	5.759	5.648	[20]
$p-\bar{p}$ <sup>(c)</sup>	155±20	155.3	147.8	[19]
$K^+/K^-$	1.8±0.1	1.652	1.700	[21]
$\bar{\Lambda}/\Lambda$	0.2±0.04	0.188	0.016	[21]

<sup>a</sup> Defined as  $\pi^- + K^- + \bar{p}$

<sup>b</sup> Includes feeding from  $\Xi$

<sup>c</sup> Measured with the '+ -' method, in this case limited rapidity acceptance (0.2-5.8) to exclude spectators

<sup>d</sup> Measured in a restricted rapidity interval and extrapolated by assuming that  $\bar{p}$  has the same rapidity distribution as the  $\bar{\Lambda}$

The validity of the approximated averaged formula in (8) in the presence of participant fluctuations has been checked by calculating its first order corrections according to the formulae quoted in Appendix B with the assumption of moderate Gaussian fluctuations of baryon number  $B$ , electric charge  $Q$  and volume  $V$ . The corrections have been estimated repeatedly by random variations of the correlations, assumed to be positive, between  $B$ ,  $Q$  and  $V$  in order to find out a maximum value. Particles undergoing the most significant variations with respect to the average yield are baryons whose production increases mainly owing to terms proportional to  $(\delta V/\bar{V})$  where  $\delta V$  is the volume dispersion. Such variations turn out to be almost constant for the three kinds of collisions as a function of the relative dispersions of  $B$ ,  $Q$  and  $V$ . They are

within 5% with no volume fluctuation even for  $\delta B/\bar{B}$  and  $\delta Q/\bar{Q}$  of 30% but can raise to more than 30% if also a volume dispersion  $\delta V/\bar{V} = 30\%$  is included.

As follows from the previous discussion (see Sect. 2) and the data presented in Table 1, the relative width of baryon number distribution is expected to be around 6% and 2% for central S+S and Pb+Pb collisions, respectively. For these participant fluctuations the corrections to baryon yields range from about 2.5% (1%) for  $\delta V/\bar{V} = 10\%$  up to 17% (13%) for  $\delta V/\bar{V} = 30\%$  in S+S (Pb+Pb) collisions. It is worth remarking that the  $B$ ,  $Q$  and  $V$  fluctuations would mainly influence the determination of the baryochemical potential in the fit as antibaryons and other particles production are much less affected by them compared with baryons.

Whilst S+S and Pb+Pb collisions involve two identical nuclei, S+Ag is an asymmetric nuclear collision and the use of the (9) to determine strange and electrical chemical potentials may be not appropriate. According to (9) the average ratio  $Q/B$  of participant nucleons in S+Ag collisions is about 0.45 whereas it is actually likely to be somewhat higher owing to the fact that Sulphur ( $Z/A=0.5$ ) is the smaller nucleus. In order to prove that our results are independent of the previous assumption, we repeated the fit by varying the charge/baryon number ratio and taking the extreme case  $Q/B=0.5$ . We found  $T = 177.5 \pm 7.9$  MeV,  $\bar{V}T^3 \exp(-0.7\text{GeV}/T) = 6.37 \pm 0.47$ ,  $\gamma_S = 0.707 \pm 0.063$ ,  $\bar{\mu}_B/T = 1.325 \pm 0.081$  with a  $\chi^2/NDF = 7.0/2$ , a fit result not significantly different from that quoted in Table 2.

A further technical problem in the  $\chi^2$  fit is concerned with data redundancy. Whenever two or more data points are in a relationship that is not dependent on any free parameter, then the  $\chi^2$  significance might be questionable as the effective number of degrees of freedom is overestimated. This is the case for S+S collisions where the (approximate) relation  $\langle K_s^0 \rangle = (\langle K^+ \rangle + \langle K^- \rangle)/2$ , owing to isospin symmetry and independent of model parameters, links three data points. However, it can be shown (see Appendix D), that such redundancy does not affect the extraction of thermal parameters nor their errors; its main effect is a lowering of the  $\chi^2/NDF$ .

Our analysis is done in the ideal pointlike hadron gas framework. Since the extracted temperatures are very high, corrections due to particle repulsion in principle should be considered. However, most corrections proposed in literature leave particle ratios unchanged [9] so that the parameters  $T$ ,  $\gamma_S$  and chemical potentials are unaffected. On the other hand, our volume parameter  $V$  is the pointlike particle volume and should not be confused with the actual volume. In a recent analysis [24] different particle ratios were compared with the full-equilibrium hadron gas predictions by introducing different hard-core radii for pions and other hadrons leading to an effective pion chemical potential. Such a procedure restores the agreement of the pion abundance which is always underestimated using thermal parameters extracted from the remaining hadrons [25] in a full-equilibrium model. However, the price to be

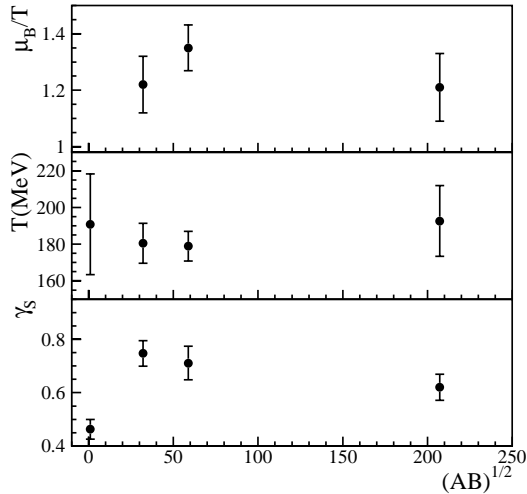


**Fig. 2.** Intensive thermal fit parameters as a function of system size. Also plotted  $T$  and  $\gamma_S$  fitted in p + p collisions at  $\sqrt{s} = 19.5$  GeV [8]

paid is the introduction of additional, particle-species dependent, parameters.

Our numerical results are quite different from a previous analysis of S+S collisions [25] which found  $T = 205 \pm 39$  MeV,  $\gamma_S = 0.95 \pm 0.20$  and  $\mu_B/T = 1.30 \pm 0.17$  by excluding negatively charged hadrons from the analysed data set. The fact that  $\chi^2/NDF > 3$  in S+S collisions is expected to produce fluctuations larger than  $1\sigma$  in the fitted parameters if some data points are excluded in turn from the fit. In fact, by excluding negatives we found  $T = 200 \pm 10$  MeV,  $\gamma_S = 0.99 \pm 0.11$  and  $\mu_B/T = 1.35 \pm 0.09$ , quite in agreement with [25]. The remaining difference can be explained by the use of an updated data sample and particularly by the inclusion, in our analysis, of resonance widths; this especially enhances the  $\rho$  meson production and, consequently, the pion production improving the agreement with the measured negatively charged hadron multiplicity.

Another recent analysis [26] of hadron abundances in Pb+Pb collisions found  $\gamma_S = 0.9 \pm 0.09$  but with the use of only strange baryons ratios in a limited phase space region and omitting the  $\phi$  multiplicity.

## 4 Discussion and conclusions

The data on hadron multiplicities in central A+A collisions at SPS energies can not be reproduced by an ideal hadron gas assuming complete chemical equilibrium. This statement is also true for the central collisions of the heaviest nuclei, Pb+Pb. The hadron gas model supplemented with partial strangeness saturation agrees significantly better with the data as the  $\chi^2/NDF$  reduces from about 7 to about 3 for S+S and S+Ag collisions and about 1 for Pb+Pb collisions.

The behaviour of the intensive parameters obtained within the off-equilibrium model is shown as a function

of the system size in Fig. 2 where the result for the p + p data at similar collision energy [8] is also included.

The lack of complete strangeness equilibrium at hadron level for central A+A collisions can not be interpreted as an effect of the choice of weights  $w(\mathbf{Q}_1^0, \dots, \mathbf{Q}_N^0)$  described in Sect. 2 which is crucial to reduce the number of free parameters. Since  $\gamma_S$  turns out to be  $< 1$ , it might be argued indeed that if the hadron gas fireballs were small enough and all with zero strangeness (so that the weights  $w(\mathbf{Q}_1^0, \dots, \mathbf{Q}_N^0)$  would be no longer those chosen in Sect. 2), a suitable canonical suppression [6, 8] could be generated without the need of  $\gamma_S$  and a hadron gas in full chemical equilibrium would be recovered. Nevertheless this mechanism would have no effect on the yield of  $\phi$  meson which is completely neutral, thus not suppressed by quantum number conservation at hadron level and having no known feeding from heavier light-flavoured resonances. Therefore, the measurement of  $\phi$  production in Pb+Pb collisions establishes the necessity of a significant strangeness suppression at hadronic level independently of the validity of the assumed fireball quantum configurations occurrence probabilities.

An important conclusion can be drawn from the resulting chemical freeze-out temperature, which seems to be independent of the system size and it is, within errors, much the same as that in  $e^+ + e^-$ , p + p and p +  $\bar{p}$  collisions [7, 8, 27]. This seems to indicate that the chemical freeze-out occurs close to the hadronization point and that the same mechanism of statistical hadronic phase space filling at critical parameters of the prehadronic matter invoked as a natural explanation of elementary collisions results [8, 27] also holds for heavy ion collisions. Moreover, the similar  $\mu_B/T$  values for all studied A+A collisions suggest a common hadronization nuclear density.

As the fit is not perfect in S+S and S+Ag collisions even in the off-equilibrium model, one may speculate that the small deviations from model predictions are due to secondary inelastic interactions between hadrons following the hadronization stage. While thought to be absent in p + p collisions, they may likely occur in A+A collisions where they can destroy the statistical character of the hadronization process. In fact, as inelastic cross sections for different processes are significantly different, hadron rescatterings may lead to decoupling of different particle species at different temperatures, thus affecting the single temperature fit. This mechanism is particularly well-suited to explain the observed deviation of antiprotons which may quickly annihilate in the baryon-dense medium formed in an A+A collision. On the other hand it should be mentioned that the observed small deviations from the off-equilibrium version of the hadron gas model could simply stem from errors in the extrapolation procedures, from participant and volume fluctuations (as described in Sect. 3) and from the choice of weights  $w(\mathbf{Q}_1^0, \dots, \mathbf{Q}_N^0)$  (see Sect. 2).

Whilst the temperature is constant, the strangeness suppression factor increases from about 0.45 for p + p interactions to about 0.7 for central S+S collisions at comparable nucleon-nucleon centre of mass energies. No further

**Table 2.** Hadron gas model fitted parameters. The first set of parameters has been obtained with a three-parameter fit by setting  $\gamma_S = 1$ . The second set is the four-parameter fit result when only experimental errors are used (first step of the fitting procedure) while the last set is the final result including uncertainties on masses, widths and branching ratios. Also quoted are the obtained chemical potentials, the matrix  $A^{-1}$  elements and the  $\chi^2$ . The  $\chi^2$  for S+S collisions within brackets is its corrected estimate accounting for kaons data redundancy (see text)

Parameter	S+S	S+Ag	Pb+Pb
$T$ (MeV)	208.3±10.4	179.9±7.8	125.4±4.6
$\bar{V}T^3 \exp[-0.7\text{GeV}/T]$	2.782±0.091	4.91±0.30	13.1±1.1
$\gamma_S$ (fixed)	1	1	1
$\bar{\mu}_B/T$	1.145±0.066	1.470±0.080	2.404±0.14
$\chi^2/\text{dof}$	34.0/5	22.3/3	22.5/4
$T_0$ (MeV)	182.4±9.2	181.8±6.9	192.6±8.1
$\bar{V}_0T_0^3 \exp[-0.7\text{GeV}/T_0]$	3.51±0.15	6.20±0.45	24.3±1.6
$\gamma_{S0}$	0.732±0.038	0.727±0.057	0.616±0.043
$\bar{\mu}_{B0}/T_0$	1.248±0.074	1.365±0.072	1.207±0.071
$\chi_0^2/\text{dof}$	17.1/4	7.74/2	3.99/3
$T$ (MeV)	180.5±10.9	178.9±8.1	192.6±19.3
$\bar{V}T^3 \exp[-0.7\text{GeV}/T]$	3.48±0.16	6.29 ±0.47	24.3±2.2
$\gamma_S$	0.747±0.048	0.711±0.063	0.620±0.049
$\bar{\mu}_B/T$	1.22±0.10	1.350±0.081	1.21±0.12
$\chi^2/\text{dof}$	12.4/4 (11.9/3)	6.44/2	3.16/3
$\bar{\mu}_S/T$	-0.320	-0.363	-0.372
$\bar{\mu}_Q/T$	-0.00217	-0.0316	-0.0655
$A^{-1}$	$(-2.00 \div 6.25)10^{-2}$	$(-1.10 \div 3.54)10^{-2}$	$(-0.30 \div 0.87)10^{-2}$

increase of the strangeness suppression factor is observed for central Pb+Pb collisions. This observation has two important consequences: firstly, a heavy ion collision is not the result of an incoherent sum of nucleon collisions as far as strangeness production is concerned. In fact, due to isospin symmetry,  $\gamma_S$  must be the same in  $p + p$  and  $n + n$  collisions at the same  $\sqrt{s}$ ; strangeness production in  $p + n$  interactions was measured to be the same as in  $p + p$  interactions [28], thus the neutron content of colliding nuclei cannot account for the increase of  $\gamma_S$  with respect to  $p + p$  and  $p + \bar{p}$  collisions. Secondly, as canonical strangeness suppression was taken into account in extracting  $\gamma_S$  in [8] and in the present analysis, the strangeness enhancement in heavy ion collisions cannot be fully attributed to the increased system size at hadron level.

The relative production of strangeness has been intensively studied in elementary [29] and nuclear collisions [30,31]. It is usually expressed in terms of a strangeness suppression factor  $\lambda_S$  defined as:

$$\lambda_S = \frac{\langle s\bar{s} \rangle}{0.5(\langle u\bar{u} \rangle + \langle d\bar{d} \rangle)}, \quad (10)$$

where  $\langle s\bar{s} \rangle$ ,  $\langle u\bar{u} \rangle$  and  $\langle d\bar{d} \rangle$  are the mean multiplicities of newly produced valence quark-antiquark pairs at primary hadron level, before resonance decays. Thus the initial colliding valence quarks are excluded in calculating  $\lambda_S$ . A major problem in the experimental determination of  $\lambda_S$  is to account for unmeasured hadron abundances. The statistical model used in this analysis is a useful tool for this pur-

pose because it reproduces well all measured hadron abundances both in elementary and nuclear collisions, thus providing a reliable quark counting method. In Fig. 3  $\lambda_S$  obtained by using model predictions for primary hadron multiplicities in  $e^+ + e^-$ ,  $p + p$ ,  $p + \bar{p}$  collisions with the parameters quoted in [27] and for A+A collisions is shown. It should be mentioned that in  $e^+ + e^-$  collisions the leading strange quarks in  $e^+e^- \rightarrow s\bar{s}$  events have been subtracted from the numerator of (10) so that  $\lambda_S$  contains only valence quarks created during the hadronization process. The  $\lambda_S$  values for elementary collisions are consistent with a constant value of about 0.2, even for very high energy  $p + \bar{p}$  collisions. The difference between  $\gamma_S$  in  $e^+ + e^-$  ( $\simeq 0.7$ ) compared to  $p + p$ ,  $p + \bar{p}$  collisions (0.46 ÷ 0.56) as resulting from the off-equilibrium hadron gas model fit [7,8] is mainly due to two effects. As far as  $p + p$  collisions are concerned, the presence of six initial  $u$ ,  $d$  quarks to be hadronized along with those newly produced brings about a  $\gamma_S$  decrease. In fact, for constant  $T$ ,  $V$  and  $\gamma_S$ , a hadron gas with increasing baryon number and electric charge, i.e. increasing number of initial protons, has an increasing  $\lambda_S$  (see Fig. 4). The physical reason is the lower energy threshold for strange pair production in a baryon rich environment where the dominant process is via  $N + \pi \rightarrow \Lambda + K$  while in the baryon free case it proceeds via kaon pair production. Secondly,  $T$  and  $\gamma_S$  are anticorrelated in  $e^+ + e^-$  collisions. As the central fitted  $T$  value is lower in  $e^+ + e^-$  collisions in comparison with  $p + p$  and  $p + \bar{p}$  collisions [27], the central  $\gamma_S$  value is ex-

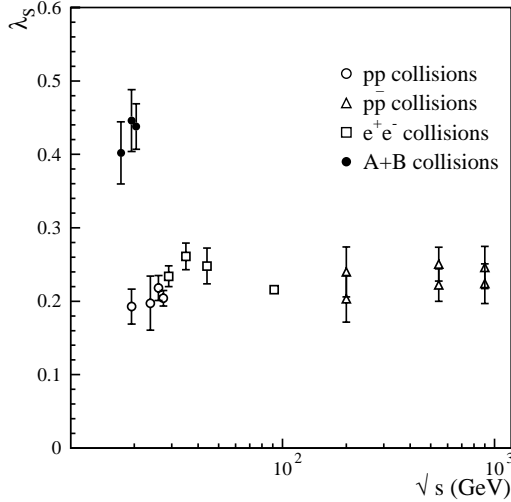


**Fig. 3.** The strangeness suppression factor  $\lambda_S = 2\langle s\bar{s} \rangle / (\langle u\bar{u} \rangle + \langle d\bar{d} \rangle)$  in high energy collisions as a function of centre of mass energy (nucleon–nucleon centre of mass energy for heavy ion collisions) calculated within the off–equilibrium hadron gas model. For  $e^+ + e^-$ ,  $p + p$  and  $p + \bar{p}$  collisions the ratios have been calculated by using model parameters quoted in [27]. For  $p + \bar{p}$  in order to estimate the possible influence of the annihilation process, we plotted in addition the  $\lambda_S$  value calculated by including initial valence quarks and antiquarks (*lower points*). For  $e^+ + e^-$  collisions the leading  $s$  quarks in  $e^+e^- \rightarrow s\bar{s}$  have been subtracted to calculate  $\lambda_S$

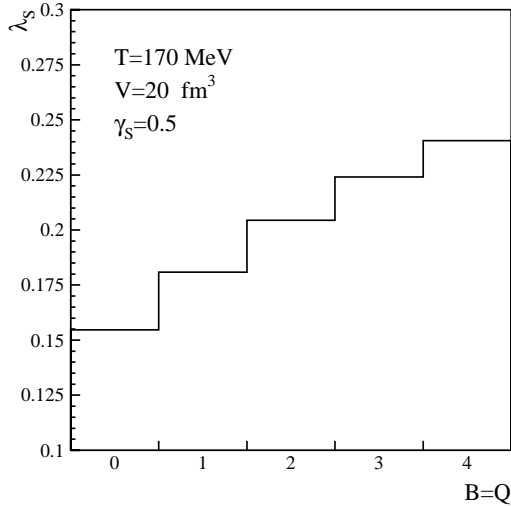


**Fig. 4.** The strangeness suppression factor  $\lambda_S = 2\langle s\bar{s} \rangle / (\langle u\bar{u} \rangle + \langle d\bar{d} \rangle)$  in a hadron gas at fixed  $T$ ,  $V$  and  $\gamma_S$  as a function of the number of initial protons (baryon number equal to electric charge)

pected to be higher in  $e^+ + e^-$  collisions to reproduce the measured strange hadron multiplicities. In fact, by repeating the same fit as in [7] for  $e^+ + e^-$  collisions at  $\sqrt{s} = 29$  and 91.2 GeV, and keeping fixed  $T = 170$  MeV instead of 160.3 MeV and 163.4 MeV respectively,  $\gamma_S$  turns out to be 0.69 and 0.62 instead of 0.72 and 0.67 respectively with a slightly worse  $\chi^2$ . Our extracted value  $\lambda_S$  is in agreement with a previous estimate based on quark counting method quoted in [32] only for energies  $\sqrt{s} < 100$  GeV. On the

other hand, the rise of  $\lambda_S$  in  $p + \bar{p}$  collisions claimed in [32, 33] is not observed. The reason of this discrepancy is the fact that  $\lambda_S$  was estimated in [33] by using only  $K/\pi$  ratio as experimental input and two parametrizations of hadron multiplicities [34, 35] which, unlike our parametrization [7, 8], do not satisfactorily reproduce all available measured multiplicities in  $p + \bar{p}$  collisions<sup>2</sup>.

To summarize, the common characteristics of elementary interactions seems to be the independence of  $\lambda_S$  on the collision energy, in the range examined in [7, 8] and type of colliding particles. This universal behaviour is broken in central A+A collisions. The value of  $\lambda_S$  turns out to be about a factor two larger than the corresponding value for elementary interactions. Our value for A+A collisions is consistent with previous estimates based on quark counting method [30]. Note that in [30]  $\lambda_S$  was also estimated for p+A collisions and found to be consistent with that of p + p collisions and independent of the size of the target nucleus. This leads to the conclusion that no strangeness enhancement is observed in p+A collisions.

The saturation of  $\gamma_S$  and  $\lambda_S$  factors as a function of the colliding system size for central A+A collisions suggests that the strangeness enhancement with respect to elementary collisions may already occur in the prehadronic phase and that secondary hadron scatterings, expected to be much more abundant in Pb+Pb collisions, are of minor importance for strangeness production. The strangeness enhancement effect observed in central A+A collisions and its independence of the colliding system size has been interpreted as due to Quark–Gluon Plasma formation in the early stage of the collision [31, 36] already in S+S collisions and not only in central Pb+Pb collisions according to the interpretation of  $J/\psi$  suppression [37, 38].

*Acknowledgements.* J.S. acknowledges the support by the Bundesministerium für Bildung und Forschung (BMBF) grant no. 06 BI 804 (5). We gratefully acknowledge helpful discussions with J. Rafelski, H. Satz and R. Stock.

## Appendix A: Rapidity distributions and statistical weights

In order to show that forward–backward peaked rapidity distributions for baryons and centrally peaked for antibaryons are not inconsistent with the assumption of statistical weights of (3) we consider a simple example of p + p collisions. Since the derived expression of average multiplicities in (4,5) does not depend either on the number of fireballs or their particular volumes  $V_1, \dots, V_N$ , we consider a toy model with three fireballs with equal volume  $V_f$  and sorted by boost velocities  $\beta_1 > \beta_2 > \beta_3$ . According to the statistical choice of weights  $w(\mathbf{Q}_1^0, \dots, \mathbf{Q}_N^0)$ , owing to the equality of all parameters  $V_i$ ,  $T_i$  and  $\gamma_{Si}$  of the

<sup>2</sup> For instance, for  $p + \bar{p}$  collisions at  $\sqrt{s} = 546$  GeV, the parametrization in [34] predicts a  $\Lambda/K_s^0$  ratio of 0.49, taking the  $\lambda_S = 0.28$  value quoted in [33], whereas the experimental value is  $0.24 \pm 0.05$



fireballs, the probability of occurrence of baryon number configurations  $\{1, 0, 1\}$ ,  $\{0, 1, 1\}$  and  $\{1, 1, 0\}$  is equal; the same holds for more complex and less probable sets of configurations such as  $\{2, 0, 0\}$ ,  $\{0, 0, 2\}$  and  $\{0, 2, 0\}$ . Therefore, as far as average hadron multiplicities are concerned, nothing changes if one replaces  $\{0, 1, 1\}$  and  $\{1, 1, 0\}$  with  $\{1, 0, 1\}$  and  $\{0, 2, 0\}$  with  $\{2, 0, 0\}$  in a half event sample and with  $\{0, 0, 2\}$  in the remaining half. The hadron abundances do not vary and a strongly forward–backward peaked rapidity distribution for baryons can be obtained as the fireballs having a non–vanishing baryon number, are always those in the forward or backward directions.

In general this argument can be repeated for  $N$  fireballs having an equal rest frame volume and an arbitrary set of ordered boost velocities  $\beta_1 > \dots > \beta_N$ . In this case the weights in (3) are symmetric:

$$w(\mathbf{Q}_{\sigma(1)}^0, \dots, \mathbf{Q}_{\sigma(N)}^0) = w(\mathbf{Q}_1^0, \dots, \mathbf{Q}_N^0) \quad (11)$$

for any permutation  $\sigma$  of the integers  $1, \dots, N$ . Therefore, if  $p(\mathbf{Q}_1^0, \dots, \mathbf{Q}_N^0)$  are the actual weights, for (5) to be valid, the condition to be fulfilled is:

$$w[\mathbf{Q}_1^0, \dots, \mathbf{Q}_N^0] = \frac{1}{N!} \sum_{\sigma} p(\mathbf{Q}_{\sigma(1)}^0, \dots, \mathbf{Q}_{\sigma(N)}^0), \quad (12)$$

where the square brackets mean that the set  $[\mathbf{Q}_1^0, \dots, \mathbf{Q}_N^0]$  is a not–ordered one. This condition is weaker than a strict equality between  $w(\mathbf{Q}_1^0, \dots, \mathbf{Q}_N^0)$  and  $p(\mathbf{Q}_1^0, \dots, \mathbf{Q}_N^0)$ .

To summarize, the compatibility between the expression for hadron multiplicities ((4,5)) and rapidity distributions can be achieved by choosing a model in which all fireballs have the same volume. Their boost velocities and their total number are allowed to vary event by event and can be determined by using actual hadron spectra.

## Appendix B: Participant nucleons and volume fluctuations

In this section we point out the conditions to be fulfilled for the replacement of (7) with its averaged version (8) in the presence of fluctuations of participant nucleons. In general, the variation of the number of participants imply fluctuations of total baryon number  $B$ , electric charge  $Q$  and also global volume  $V$  of the colliding system. We assume that the associated distribution function  $F(Q, B, V)$  is a Gaussian one and that the mean values  $\bar{Q}$  and  $\bar{B}$  are large, which is the case in the examined collisions. If the latter condition is met, the sum over quantum vectors  $\mathbf{Q}^0$  in (7) can be turned into an integration:

$$\begin{aligned} \langle n_j \rangle &= (2J_j + 1) \frac{T}{2\pi^2} \sum_{l=1}^{\infty} (\mp 1)^{l+1} \gamma_S^{ls_j} \frac{m_j^2}{l} K_2 \left( \frac{lm_j}{T} \right) \\ &\times \int dQ dB dV F(Q, B, V) V \\ &\times e^{l\boldsymbol{\mu} \cdot \mathbf{q}_j / T} e^{-l^2 \mathbf{q}_j \mathbf{A}^{-1} \mathbf{q}_j / 4}. \end{aligned} \quad (13)$$

No more factor can be drawn out of the integral as the chemical potentials  $\boldsymbol{\mu}$  depend on the integration variables

because of the quantum number conservation constraint  $\sum_j \mathbf{q}_j \langle n_j \rangle = \mathbf{Q}^0$  and the matrix  $\mathbf{A}$  is proportional to the volume (see (6)). Nevertheless, they can be expanded off the mean values  $\bar{Q}$ ,  $\bar{B}$  and  $\bar{V}$  up to first order, provided that the dispersions are not too large:

$$\begin{aligned} \boldsymbol{\mu} &\simeq \boldsymbol{\mu}(\bar{\mathbf{X}}) + \mathbf{J}_{\boldsymbol{\mu}}(\mathbf{X} - \bar{\mathbf{X}}) \\ \mathbf{A}^{-1} &\simeq \bar{\mathbf{A}}^{-1} + \frac{\partial \mathbf{A}^{-1}}{\partial V} (V - \bar{V}) = \bar{\mathbf{A}}^{-1} \left( 1 - \frac{V - \bar{V}}{\bar{V}} \right). \end{aligned} \quad (14)$$

where  $\mathbf{X} = (\bar{Q}, \bar{B}, \bar{V})$  and  $\mathbf{J}$  is the Jacobian matrix. Using the above expansions in (14) one obtains:

$$\begin{aligned} \langle n_j \rangle &= \sum_{l=1}^{\infty} \langle n_j \rangle_l \int dQ dB dV \left( 1 + \frac{V - \bar{V}}{\bar{V}} \right) F(Q, B, V) \\ &\times \exp \left[ l \mathbf{q}_j \cdot \mathbf{J}_{\boldsymbol{\mu}}(\mathbf{X} - \bar{\mathbf{X}}) / T + l^2 \mathbf{q}_j \bar{\mathbf{A}}^{-1} \frac{(V - \bar{V})}{\bar{V}} \mathbf{q}_j / 4 \right] \end{aligned} \quad (15)$$

where  $\langle n_j \rangle_l$  is just the  $l^{\text{th}}$  term of the series in (8). The second term in the exponential is negligible if we are close to the grand-canonical regime and if the temperature is low enough to quickly suppress the terms of the series with high  $l$ : this condition is met for all hadrons if  $T < 200$  MeV. Therefore:

$$\begin{aligned} \langle n_j \rangle &\simeq \sum_{l=1}^{\infty} \langle n_j \rangle_l \int dQ dB dV \left( 1 + \frac{V - \bar{V}}{\bar{V}} \right) \\ &\times F(Q, B, V) \exp[l \mathbf{q}_j \cdot \mathbf{J}_{\boldsymbol{\mu}}(\mathbf{X} - \bar{\mathbf{X}}) / T]. \end{aligned} \quad (16)$$

If  $F$  is a multivariate Gaussian:

$$F(\mathbf{X}) = \frac{1}{\sqrt{(2\pi)^3 \det \mathbf{C}}} \exp[-(\mathbf{X} - \bar{\mathbf{X}}) \cdot \mathbf{C}^{-1} (\mathbf{X} - \bar{\mathbf{X}}) / 2], \quad (17)$$

then the integral in (16) can be solved analytically if the integration is extended to infinity. This is a satisfactory approximation if the dispersions are small compared to the mean values, which is one of the basic requirements mentioned above.

$$\begin{aligned} \langle n_j \rangle &\simeq \sum_{l=1}^{\infty} \langle n_j \rangle_l \left[ 1 + \frac{l}{T\bar{V}} (\mathbf{C} \mathbf{J}_{\boldsymbol{\mu}}^T \mathbf{q}_j)_3 \right] \\ &\times \exp \left[ l^2 \mathbf{q}_j \cdot \mathbf{J}_{\boldsymbol{\mu}} \mathbf{C} \mathbf{J}_{\boldsymbol{\mu}}^T \mathbf{q}_j / (2T^2) \right]. \end{aligned} \quad (18)$$

Thus, for the approximation (8) to be valid, it is necessary that  $\mathbf{C} \mathbf{J}_{\boldsymbol{\mu}}^T / (T\bar{V}) \ll 1$  and  $\mathbf{J}_{\boldsymbol{\mu}} \mathbf{C} \mathbf{J}_{\boldsymbol{\mu}}^T / T^2 \ll 1$ . The Jacobian matrix  $\mathbf{J}_{\boldsymbol{\mu}}$  can be calculated by taking the derivative of the quantum numbers conservation constraint:

$$\frac{\partial}{\partial Q_i^0} \sum_j \mathbf{q}_j n_j = \sum_j \mathbf{q}_j \sum_{l=1}^{\infty} n_{jl} \frac{l}{T} \sum_k q_j^k \frac{\partial \mu^k}{\partial Q_i^0} = \mathbf{e}_i, \quad (19)$$

where  $\mathbf{e}_i$  is the  $i^{\text{th}}$  unitary vector. If we define the matrix  $\mathbf{B}$ :

$$\mathbf{B}_i^k = \sum_j \sum_{l=1}^{\infty} l n_{jl} q_j^k q_j^i, \quad (20)$$

then the righthand equality in (19) can be inverted so to obtain the derivatives of the chemical potentials:

$$\frac{\partial \mu^k}{\partial Q_i^0} = T (\mathbf{B}^{-1})_i^k. \quad (21)$$

It should be noted that the matrix  $\mathbf{B}$  would be equal to  $2\mathbf{A}$  if  $\boldsymbol{\mu}/T = 0$ . Since  $\boldsymbol{\mu}/T$  is generally  $\mathcal{O}(1)$  it turns out that  $\mathbf{B}^{-1} = \mathcal{O}(\mathbf{A}^{-1})$ , hence it is expected to be much smaller than 1. To complete the Jacobian matrix  $\mathbf{J}_\mu$ , we take the derivative of the quantum numbers conservation constraint with respect to  $V$  for  $V = \bar{V}$ , yielding:

$$\frac{\mathbf{B} \partial \boldsymbol{\mu}}{T \partial \bar{V}} + \frac{\mathbf{Q}^0}{\bar{V}} - \frac{1}{4\bar{V}} \sum_j \sum_{l=1}^{\infty} l^2 \mathbf{q}_j \bar{\mathbf{A}}^{-1} \mathbf{q}_j n_{jl} = 0. \quad (22)$$

We use the Boltzmann limit for all hadrons in the last term, namely we keep only the first term of the series. By using this approximation, which is satisfactory if  $T \simeq 170$  MeV, we conclude that the last term is  $\simeq (1/4)\mathbf{B}^{-1}\mathbf{Q}^0/\bar{V}$  which is much less than  $\mathbf{Q}^0/\bar{V}$ . Therefore:

$$\frac{\partial \boldsymbol{\mu}}{\partial \bar{V}} \simeq -T\mathbf{B}^{-1} \frac{\mathbf{Q}^0}{\bar{V}}. \quad (23)$$

Finally, the Jacobian matrix  $\mathbf{J}_\mu$  turns out to be:

$$\mathbf{J}_\mu \simeq T(\mathcal{O}(\mathbf{A}^{-1}), \mathcal{O}(\mathbf{A}^{-1}), \mathcal{O}(\mathbf{A}^{-1}\mathbf{Q}^0/\bar{V})), \quad (24)$$

where each term is meant to be a column vector. This result can be used in conjunction with the (18) to establish the validity of the approximation (8). If  $\mathbf{A}^{-1} \ll 1$  moderate fluctuations of  $B$ ,  $Q$ ,  $V$  in comparison with the mean values are needed in order that  $\mathbf{C}\mathbf{J}_\mu^T/T\bar{V} \ll 1$  and  $\mathbf{J}_\mu \mathbf{C}\mathbf{J}_\mu^T/T^2 \ll 1$ .

## Appendix C: Fitting procedure

We adopted a two-step fit procedure to also take into account the uncertainties on input parameters such as hadron masses, widths and branching ratios, which in principle can play a significant role in the test of the model. Firstly a  $\chi^2$  with only experimental errors has been minimized and preliminary best-fit model parameters  $T_0$ ,  $\bar{V}_0$ ,  $\bar{\mu}_{B0}$  have been determined:

$$\chi^2 = \frac{\sum_{i=1}^M (y_i^{\text{exp}} - y_i^{\text{theo}})^2}{\sigma_i^2}, \quad (25)$$

where the index  $i$  runs over the  $M$  data points. Keeping the preliminary model parameters fixed, the variations  $\Delta y_i^{\text{theo}}$  of the multiplicities (or ratios) corresponding to the variations of the  $l^{\text{th}}$  input parameter by one standard deviation have been calculated. Such variations have been considered as additional systematic uncertainties on the multiplicities and the following covariance matrix has been formed:

$$C_{ij}^{\text{sys}} = \sum_l \Delta y_i^l \Delta y_j^l \quad (26)$$

to be added to the experimental covariance matrix  $C^{\text{exp}}$ . Finally a new  $\chi^2$  has been minimized:

$$\chi^2 = \sum_{i,j=1}^M (y_i^{\text{exp}} - y_i^{\text{theo}})[(C^{\text{exp}} + C^{\text{sys}})^{-1}]_{ij} (y_j^{\text{exp}} - y_j^{\text{theo}}) \quad (27)$$

from which the best-fit estimates of the model parameters and their errors have been obtained. Actually more than 130 among the most significant or worst known input parameters have been considered and the corresponding  $1\sigma$  variations performed. This fit technique upgrades the one used by one of the authors in the analysis of thermal hadron production in  $e^+ + e^-$ ,  $p + p$  and  $p + \bar{p}$  collisions [6–8] in that the off-diagonal elements of  $C^{\text{sys}}$  are also included.

## Appendix D: $\chi^2$ and data redundancy

We prove that the parameters fitted with a  $\chi^2$  minimization and their errors are not affected by the presence of redundant data. Let  $y_1 \dots y_N$  be a set of experimental measurements among which  $y_k \dots y_N$  are measurements of the same variable. Let  $y = f(x, \mathbf{a})$  be the functional dependence to be tested where  $\mathbf{a}$  is a set of parameters to be determined by means of a  $\chi^2$  minimization:

$$\chi^2 = \sum_{i=1}^N \frac{(y_i - f(x_i, \mathbf{a}))^2}{\sigma_i^2}. \quad (28)$$

The (28) can be written also:

$$\chi^2 = \sum_{i=1}^{k-1} \frac{(y_i - f(x_i, \mathbf{a}))^2}{\sigma_i^2} + \sum_{i=k}^N \frac{(y_i - \bar{y} + \bar{y} - f(x_k, \mathbf{a}))^2}{\sigma_i^2}, \quad (29)$$

where  $\bar{y}$  is the weighted average of  $y_k \dots y_N$ ; all these values correspond to the same abscissa  $x_k$ . Hence:

$$\chi^2 = \sum_{i=1}^{k-1} \frac{(y_i - f(x_i, \mathbf{a}))^2}{\sigma_i^2} + \sum_{i=k}^N \frac{(y_i - \bar{y})^2}{\sigma_i^2} + \sum_{i=k}^N \frac{(\bar{y} - f(x_k, \mathbf{a}))^2}{\sigma_i^2} + 2 \sum_{i=k}^N \frac{(y_i - \bar{y})(\bar{y} - f(x_k, \mathbf{a}))}{\sigma_i^2}. \quad (30)$$

The second term in the above equation is simply the  $\chi^2$  of the weighted average while the third term can be written  $(\bar{y} - f(x_k, \mathbf{a}))^2/\sigma_{\bar{y}}^2$ ,  $\sigma_{\bar{y}}$  being the error on the weighted average  $\bar{y}$ ; the fourth term vanishes by definition of weighted average. Therefore:

$$\chi^2 = \chi_{WA}^2 + \chi_{fit}^2, \quad (31)$$

where  $\chi_{WA}^2$  is the  $\chi^2$  of the weighted average and:

$$\chi_{fit}^2 = \sum_{i=1}^{k-1} \frac{(y_i - f(x_i, \mathbf{a}))^2}{\sigma_i^2} + \frac{(\bar{y} - f(x_k, \mathbf{a}))^2}{\sigma_{\bar{y}}^2} \quad (32)$$

is just the correct  $\chi^2$  to minimize, for the  $N - k + 1$  redundant points have been replaced with their weighted average. Since  $\chi_{WA}^2$  does not depend on  $\mathbf{a}$ , the minimization of either  $\chi^2$  or  $\chi_{fit}^2$ , the latter being the correct one, leads to the same results. On the other hand, if  $n = \dim(\mathbf{a})$  is the number of fitted parameters, the normalized  $\chi_{fit}^2$  is:

$$\chi_{fit}^2 = \frac{\chi^2 - \chi_{WA}^2}{k - n} \quad (33)$$

instead of  $\chi^2/(N - n)$ .

## References

1. for a recent review see: Proceedings of Quark Matter '96, Nucl. Phys. A610 (1996)
2. E. Fermi: Progr. Theor. Phys. 5 (1950) 570
3. L.D. Landau: Izv. Akad. Nauk SSSR, Ser. Fiz. 17 (1953) 51
4. R. Hagedorn: Nuov. Cim. 15 (1960) 434
5. Proceedings of Hot Hadronic Matter: Theory and Experiment, J. Letessier, H.H. Gutbrod, J. Rafelski (Eds.), Plenum Press, New York, 1995
6. F. Becattini: Z. Phys. C 69 (1996) 485
7. F. Becattini: Proc. of the XXXIII Eloisatron workshop on universality features in multihadron production and the leading effect, Erice(Italy) October 1996, in press, Firenze preprint DFF 263/12/1996 (hep-ph/9701275)
8. F. Becattini, U. Heinz: Z. Phys. C 76 (1997) 269 (hep-ph/9702274)
9. J. Sollfrank: Proc. of International Symposium 'Strangeness in Quark Matter 1997', Santorini (Greece), April 14 - 18, 1997, to be published in J. Phys. G (nucl-th/9707020)
10. J. Rafelski: Phys. Lett. 262B (1991) 333
11. J. Letessier, J. Rafelski, A. Tounsi: Phys. Rev. C 50 (1994) 406 C. Slotta, J. Sollfrank, U. Heinz: Proc. of Strangeness in Hadronic Matter (Tucson), J. Rafelski (Eds.), AIP Press, Woodbury 1995, p. 462
12. T. Alber et al., NA35 Collab.: Z. Phys. C 64 (1994) 195
13. A.I. Golokhvastov: Ph.D. Thesis, Dubna (1989), Dubna Report JINR 1-89-698
14. R.M. Barnett et al., Particle Data Group: Phys. Rev. D 54 (1996) 1
15. T. Alber et al., NA35 Collab.: Frankfurt University Report IKF-HENPG/6-94 (1994), submitted to Z. Phys. C (hep-ex/9711001)
16. J. Bächler et al., NA35 Collab.: Z. Phys. C 58 (1993) 367
17. T. Alber et al., NA35 Collab.: Phys. Lett. 366B (1996) 56
18. I. Huang (NA49 Collab.): Ph.D. Thesis, U.C. Davis (1997)
19. S.V. Afanasjev et al., NA49 Collab.: Nucl. Phys. A610 (1996) 188c
20. V. Friese et al., NA49 Collab.: Proc. of International Symposium 'Strangeness in Quark Matter 1997', Santorini (Greece), April 14-18, 1997, to be published in J. Phys. G
21. C. Bormann et al., NA49 Collab.: Proc. of International Symposium 'Strangeness in Quark Matter 1997', Santorini (Greece), April 14-18, 1997, to be published in J. Phys. G
22. K. Redlich, J. Cleymans, H. Satz, E. Suhonen: Nucl. Phys. A566 (1994) 391c
23. P. Braun-Munzinger, J. Stachel, J.P. Wessels, N. Xu: Phys. Lett. 365B (1996) 1
24. G.D. Yen, M.I. Gorenstein, W. Greiner, S.N. Yang: Phys. Rev. C 56 (1997) 2210 (nucl-th/9711062)
25. J. Sollfrank, M. Gaździcki, U. Heinz, J. Rafelski: Z. Phys. C 61 (1994) 659
26. J. Letessier, J. Rafelski, A. Tounsi: Paris preprint PAR-LPHE-97-25 (hep-ph 9710310), Phys. Lett. B (1997) in press
27. F. Becattini: Proc. of International Symposium 'Strangeness in Quark Matter 1997', Santorini (Greece), April 14 - 18 1997, to be published in J. Phys. G, Firenze preprint DFF 284/07/1997 (hep-ph 9708248)
28. M. Gaździcki, O. Hansen: Nucl. Phys. A52B (1991) 754
29. W. Hoffmann: Nucl. Phys. A479 (1988) 337c
30. H. Białkowska, M. Gaździcki, W. Retyk, E. Skrzypczak: Z. Phys. C 55 (1992) 347
31. M. Gaździcki, D. Röhrich: Z. Phys. C 71 (1996) 55
32. A.K. Wróblewski: Acta Phys. Pol. **B16** (1985) 379
33. A.K. Wróblewski: Proc. of the XXV International Conference on High Energy Physics, Singapore 1990, p. 125
34. V.V. Anisovich, M.N. Kobrinsky: Phys. Lett. 52B (1974) 217
35. V.M. Schekter, L.M. Scheglova: Sov. J. Nucl. Phys. 27 (1978) 567
36. M. Gaździcki: Proc. of the International Workshop XXV on Gross Properties of Nuclei and Nuclear Excitations, 'QCD Phase Transitions', Hirschegg (Austria), January 13-18 (1997), p. 217, nucl-th/9701050
37. M. Gonin et al., NA50 Collab.: Nucl. Phys. A610 (1996) 404c
38. J.P. Blaizot, J.Y. Ollitrault: Nucl. Phys. A610 (1996) 452c D. Kharzeev: Nucl. Phys. A610 (1996) 418c